Proceedings of the Seventeenth (2007) International Offshore and Polar Engineering Conference
Lisbon, Portugal, July 1-6, 2007

ISBN 978-1-880653-68-5; ISBN 1-880653-68-0(Set); ISSN 1098-6189 (Set)

A Study on A Semi-Submersible Floating Offshore Wind Energy Conversion System

K. Shimada, T. Ohyama
Institute of Technology, Shimizu Corporation, Tokyo, Japan

M. Miyakawa
Design Department, Civil Engineering Technology Division, Shimizu Corporation, Tokyo, Japan

T. Ishihara
Institute of Engineering Innovation, School of Engineering, The University of Tokyo, Tokyo, Japan

P.V. Phuc
School of Engineering, The University of Tokyo, Tokyo, Japan

H. Sukegawa
R&D Center, Engineering R&D Division, Tokyo Electric Power Company, Kanagawa, Japan

ABSTRACT

A new semi-submersible floating structure is proposed on which three wind turbine towers are installed. This paper presents a basic characteristic of the wave-induced motion of this semi-submersible floating structure via. numerical computations and 1/150 scaled rigid model experiments in a wave tank. In the numerical computations, non-linear damping effect due to drag forces modeled by the Morison's formula is considered in the equation of motion, where the linear hydrodynamic forces are obtained from the Green's function model. As a result, the response characteristics around the resonant frequency region were successfully improved. In addition to such basic examination, major results of feasibility studies, including the structural stability for severe wave conditions and the long-term fatigue limit state, are presented for a realistic situation.

KEY WORDS: Offshore wind energy conversion system; Semi-submergible floater; Green's function method; Damping force; Fatigue analysis.

NOMENCLATURE

B : Width of a floater.
C_{jk} : Restoring force coefficient by hydrostatic force
C_D : Drag coefficient.
D : Reference length of a cross-section of an element.
E_j^* : Fourier component of the Wave–exciting force
$\hat{E}_j^*$: Fourier component of the Wave–exciting force
F : Fetch
G_{jk} : Mooring force coefficient
H_0 : Height of incident wave.
$H_{1/3}$: Significant wave height.
H_{SMB} : Significant wave height by SMB formula.
M_{jk} : Mass coefficient
m_{jk} : Added mass coefficient
N_{jk} : Wave making damping coefficient
$\hat{N}_{jk}$: Equivalent linear viscous damping coefficient
$T_{1/3}$: Significant wave period.
u_I : Velocity of a fluid particle perpendicular to an element.
U_S : Velocity of an element perpendicular to an element.
U_{10} : Hourly mean wind speed at 10m above the sea surface
V_{HUB} : 10 min. mean wind speed at hub height of a wind turbine
ΔF_D : Drag force component which is perpendicular to an element of length Δl.
λ : Wave length.
ρ : Density of sea water.
ξ_{jk}^* : Fourier component of the displacement

INTRODUCTION

At the end of 2005 in Japan, total amount of installed wind power capacity reached to 1,078MW. However, a large portion of wind energy potential in Japan is located at rural area, where demand is low, the grids are weak, and the limitation in integrating wind energy to the grids exists. Onshore wind resource is almost developed and little land is left for large-scale wind farm. Thus if offshore energy potential near urban area is high, it will help the penetration of wind energy in Japan. In the European countries where wind conversion systems have been developed for a long time, *Offshore Wind Energy Conversion systems* (OWEC) have already been operated. In Japan where totaling 3,000 MW installed wind capacity is officially planned to reach by 2010, realization of an OWEC is strongly expected in order to achieve the target.

Fig.1 displays a sea area where the offshore wind farm is supposed to constructed in this study and spatial distribution of annual mean wind (Sukegawa et al. 2006). Wind speeds depends on the region, however, there are some regions where wind speed is expected over 7m/s only at 10km off from coast line.

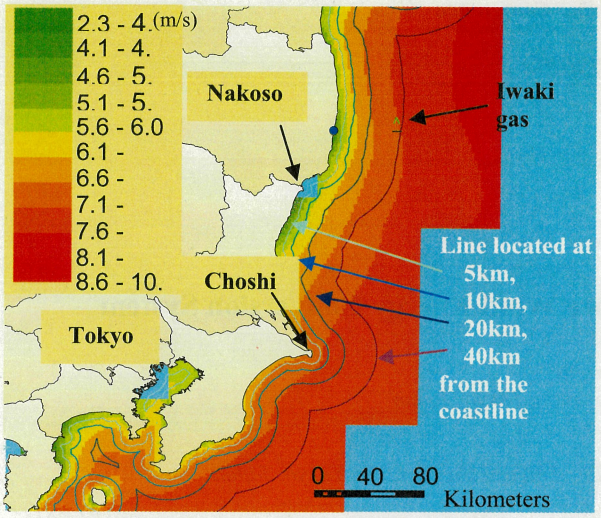

Fig. 1 Figure 5. Distribution of annual mean wind speed and the line located at 5 to 40km from the coastline (Sukegawa et al. 2006)

However, in general, sea area around Japan is heavy and water depth steeply increases. Under such circumstance, floating type OWEC is better than fixed type. Thus we have proposed a new semi-submersible floating structure. The basic designing concept was focused on reducing of construction cost and achieving of stability in order to reduce loading on wind turbine and its tower. Based on this concept, the structure is featured by large natural periods for all six degrees of freedom by adopting a weak mooring system and setting the hydrostatic restoring force as small as possible, which may significantly contributes to suppress the wave-induced motion.

This paper verifies the basic characteristic of the wave-induced motion of this semi-submersible floating structure via. numerical analysis and 1/150 scaled rigid model experiments.

FLOATING STRUCTURE

Fig.2 displays the floating structure which is discussed in this paper. On the floater, three 2.4MW wind turbines (rotor diameter of 92m and hub height of 70m) are installed. Floating structure consists of three wind turbine base floater (WBF), one central base floater (CBF), girders which connect these base floaters and mooring cables. As the mooring system, chain mooring system with three directions are employed. Each mooring line consists of three chains therefore as a whole the mooring system consists of total nine point anchored mooring. WBF is made of a composite structure from steel and concrete, and supports its weight by its buoyancy. Connection girders are made of steel and are balanced its weight with concrete ballast which is added in order to cancel its buoyancy since they are in the sea water. Furthermore, connection girders and CBF are connected with cables. The effect of the cable structure system is expected to reduce the bending moments of the girder which is generated by horizontal forces.

In order to reduce the wave induced motion, natural periods of the structure are extended as large as possible by suppressing the restoring stiffness of each 6-degrees-of-freedom motion. To put it concretely, as mooring system, intermediate sinker is introduced in order to suppress stiffness by mooring in a horizontal motion mode, i.e. surge, sway and yaw. Furthermore, water plane area of the WBF is designed to be smaller than its cross-sectional area beneath the wave in order to reduce the restoring stiffness of heave, roll and pitch mode. By these structural

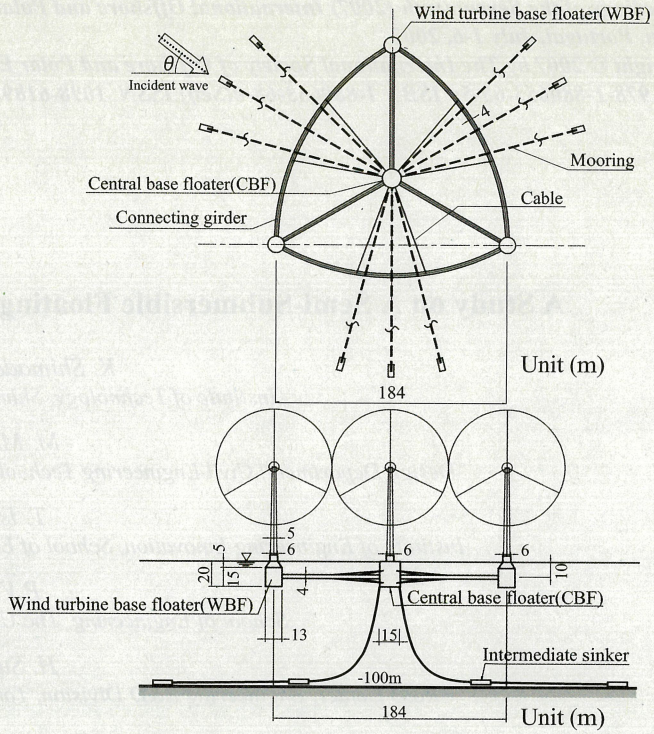

Fig. 2 A Semi-submerged floating structure for offshore wind energy production system

strategies, fundamental natural periods of above 25 seconds are achieved in for all modes.

INCORPORATION OF A DAMPING EFFECT DUE TO DRAG FORCE INTO AN ANALYTICAL MODEL FOR WAVE INDUCED MOTION

Green's Function Method

Motion of the floating structure is obtained by solving the following motion of equation in frequency domain.

$$\sum_{k=1}^{6}\left[-\omega^2\left\{M_{jk}+m_{jk}(\omega)\right\}+(-i\omega)\left\{N_{jk}(\omega)+\hat{N}_{jk}(\omega)\right\}+C_{jk}+G_{jk}\right]\xi_k^* = E_j^*(\omega)+\hat{E}_j^*(\omega) \quad (1)$$

Among the fluid dynamic forces acting on the floating structure, for estimation of wave-exciting force, added mass and wave damping coefficients, Green's function method based on the linear potential theory is applied. For the calculation of the Green's function, since the direct application of the original formulation proposed by Wehausen et al. (1960) deteriorates the numerical accuracy, a method which is transformed into a series expansion which shows a good convergence performance by Seto (1991, 1992) is applied.

In order to verify the Green's function method, comparisons were made between the model and model test by Takayama et al.(1980). Figure 3 is the result of wave induced motion in the sway, heave and roll mode. In the figure, B, λ and H_0 expresses width of a floater, wave length and wave height of the incident wave, respectively. As can be found from these figures, numerical result can reproduce the experimental results well. Furthermore for a pontoon type floater, it is also verified that the Green's function method completely agrees with the result by the model based on the expanded mild-slope equations proposed by Ohyama et al. (1997) which is based on the linear potential theory.

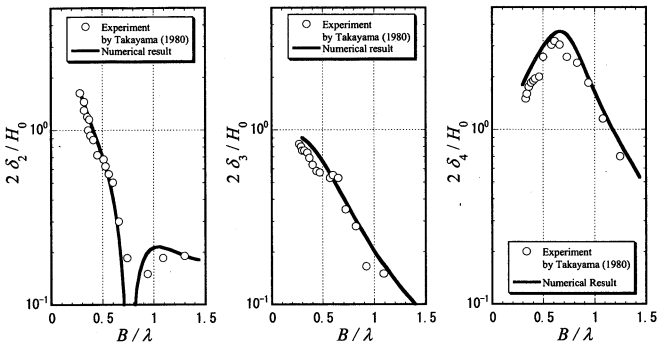

(a) Sway (b) Heave (c) Roll

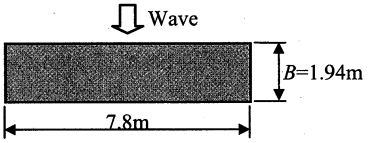

Displacement W	1.362 tf
Water plane area A	15.132 m^2
Center of gravity G	0.215 m
Roll meta center height $(GM)_{xx}$	3.22 m
Mass moment of inertia I_{xx}	0.522 tm^2
Water depth	0.52 m
Draft	0.09 m

Fig. 3 Comparison of response characteristics between the numerical and experimental results by Takayama et al. (1980)

Model for a Non-Linear Damping Force

In the ordinal numerical model for a wave induced motion which incorporates Green's function, as a mechanism of the damping, only the wave making damping force is considered. However, in the semi-submersible floating structure like in this paper which consists of a lot of structural elements with small diameter, the effect of vortex-induced drag force is regarded to be predominant. By Morrison's formula, drag forces acting on each structural element is expressed as follows,

$$\Delta F_D = \frac{1}{2}\rho C_D D|u_I - U_S|(u_I - U_S)\Delta l \tag{2}$$

where ΔF_D is drag force component which is perpendicular to an element of length Δl, ρ is density of sea water, C_D is drag coefficient, D is reference length of a cross-section of an element, u_I is velocity of a fluid particle perpendicular to an element and U_S is velocity of an element perpendicular to an element.

Since the Green's function method which is a base of the model is a frequency domain calculation method and therefore harmonic vibration is assumed, instead of using eq.(2), it is linearized as follows (Architectural Institute of Japan 1990),

$$\Delta F_D \approx \frac{1}{2}\rho C_{DL} D\,(u_I - U_S)\Delta l \tag{3}$$

$$\text{for a periodic wave}: C_{DL} = C_D \times \frac{8}{3\pi} MAX\{|u_I - U_S|\} \tag{4}$$

$$\text{for a random wave}: C_{DL} \approx C_D \times \sqrt{\frac{8}{\pi}}\, RMS\{|u_I - U_S|\} \tag{5}$$

In Fig.4, computational steps are illustrated for a calculation of a wave induced motion of a floating structure which is subjected to a random incident wave. At first, linear fluid forces are prepared by the Green's function method on a frequency domain. Here, the wave-exciting force

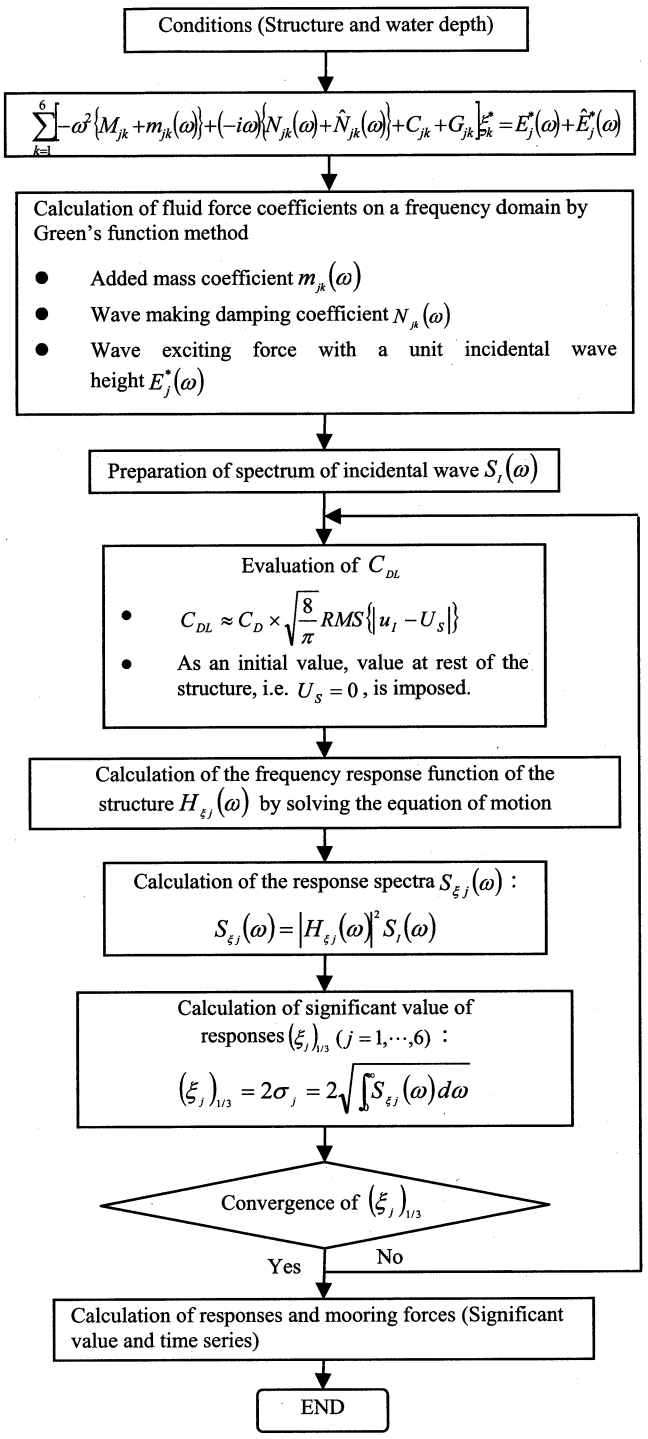

Fig. 4 Steps of calculation of wave induced motion

is calculated with a unit wave height. Next, with an initial value for the C_{DL} in eq.(5) as U_S=0 which corresponds to a floating structure at rest, wave induced motion with a unit incident wave height, i.e. frequency response function, is calculated by solving an equation of 6-degrees-of-freedom motion for a floating structure on a frequency domain eq.(1). Then from the incident wave spectrum and the response function, variances of the 6-degrees-of-freedom motion are calculated and C_{DL} in eq.(5) is evaluated for each element. With these values the wave

induced motion is calculated. The above procedure is iterated until the convergence criterion is satisfied.

MODEL TEST

Setup of the Experiment

The experiment was performed at the wave tank of National Maritime Research Institute in Japan. Its length, width and depth of the wave tank is 17.6m, 3m and 1.5m and wave generator is a flap type. Experimental model is a 1/150 scaled rigid model which is made of acryl. Here, cross-section of the connection girder is modified to a square cross section from a circle in the prototype floater for the convenience of fabrication, and the cables are not attached. In Table.1, comparisons are made between 1/150 scaled prototype floater and experimental model.

Table 1. Specifications of the experimental model

	1/150 scaled prototype floater	Experimental Model	Note
Displacement (t)	0.486×10^{-2}	0.554×10^{-2}	Diameter of WBF 1/150 scaled prototype model : $\phi_{1/150}$=0.0867m Experimental model : ϕ=0.0900m
Moment of inertia I_{xx}, I_{yy}(tm^2)	0.77×10^{-3}	0.862×10^{-3}	
Center of gravity (m)	0.060	0.048	Depth from hydrostatic surface
Height of meta-center (m)	0.171	0.171	
Waterplane area (m^2)	0.377×10^{-2}	0.377×10^{-2}	
Spring constant (kN/m)	0.196×10^{-1}	0.147×10^{-1}	

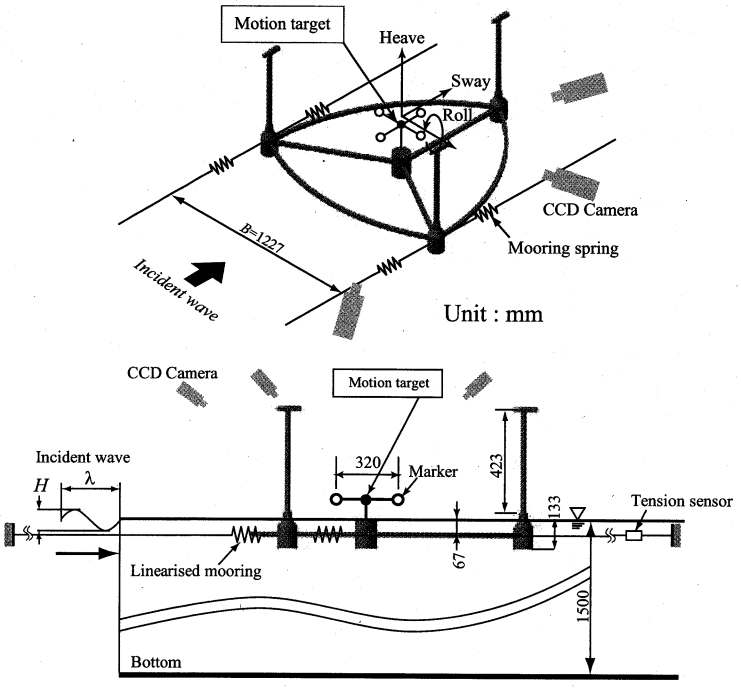

Fig. 5 Measuring of responses

Figure 5 shows a setup of measuring apparatus. Experiment was conducted for an incident wave angle of 90 degree, see Fig.2. Mooring system was modeled as a linearized horizontal spring in which its spring constant was scaled from that of a prototype floating structure at extreme wind condition. Motions of the experimental model are determined as transforming motion of five targets on a CBF, which are monitored by three CCD cameras, into displacements in 6-degrees-of freedom by means of motion picture analysis. Water depth was set as 1.5m. Incident waves are periodic with 2, 4 and 8cm wave height. Wave periods were ranged from 0.6 to 3.0 seconds. Frequency component which corresponds to the incident wave period were extracted from measured data by Fourier analysis.

Comparison between the Experimental and Numerical Result

In the computation by the Green's function method, submerged surface of the model was discretised into 1918 elements. Also, at the same time, structure was discretised into 394 beam elements so as to evaluate the drag force. Drag coefficient C_D is set as 2.0 for square cross-section elements, 1.0 for base floaters.

Figures 6, 7 and 8 demonstrates motion amplitude of each mode, i.e. sway, heave and roll, acceleration of the CBF and frequency response characteristics of the mooring system, respectively. In each figure, results in which drag force is neglected, i.e. C_D =0, are also presented. Natural periods of each mode are found to be within a range from 2.5 to 2.7 seconds, i.e. from 30 to 33 seconds in prototype floating structure, and the peaks which appeared below 1 second are generated by phase interactions among wave exciting forces acting on WBF, CBF and connection girders. For sway and heave motion, numerical results agree well with the experimental results. Especially for sway mode, dependence of frequency response on the incident wave height are clearly observed near its natural period. Response characteristics obtained from the experiment are successfully simulated. Since in the simulation in which drag force is neglected, frequency response of any mode near their natural periods are overestimated, it can be recognized that the damping effect due to drag force is predominant compared to wave making damping for this floating structure.

However, frequency response of the roll mode near its natural period is different from the experimental result in that peaks are not appeared clearly in the latter. Although the figure is not demonstrated in this paper, from the inspection of time series of the motion response, it was recognized that the sway and heave motion shows almost sinusoidal response, however, roll response near its natural period shows strong non-linearity including high frequency components even at incident wave height of 2cm. For this disagreement, a couple of reasons such as effect of elastic deformation of the experimental model, non-linearity of restoring force characteristics which is generated by changing of water plane area and underestimation of damping effect due to vertical motion of WBF can be considered. Although the numerical model tends to overestimate the roll motion, it can be regarded that the experimental results are successfully simulated by this numerical model including the vortex induced damping effect.

For reference of a convergence performance of the calculation due to linearization of the non-linear damping term, Fig.9 demonstrates a convergence of the numerical solution in the sway mode near its natural period. Ordinate shows a relative error to the solution at 1,000 iterations and results of incident wave height of 2cm and 8cm are demonstrated. Since the latter shows a stronger non-linearity, number of iteration for the same allowable error increases, it can be recognized that with 150 iterations convergence error reduces below 1 percent. Period range which is far apart from the natural period, number of iteration necessary for the convergence drastically decreases for all

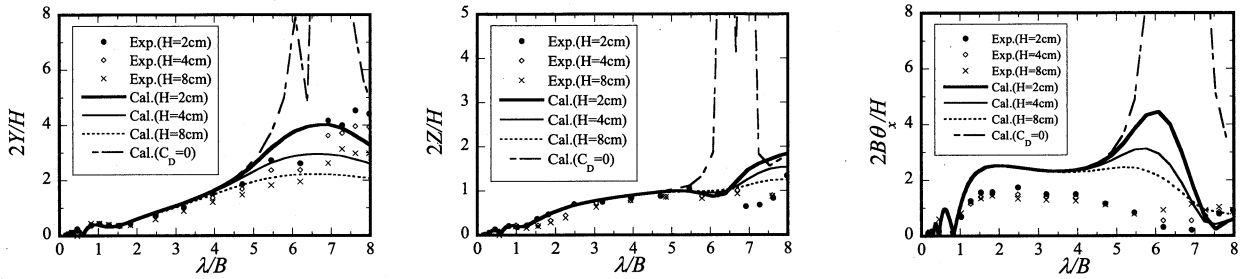

(a) Sway (b) Heave (c) Roll

Fig. 6 Comparison of displacement responses between the numerical and experimental results

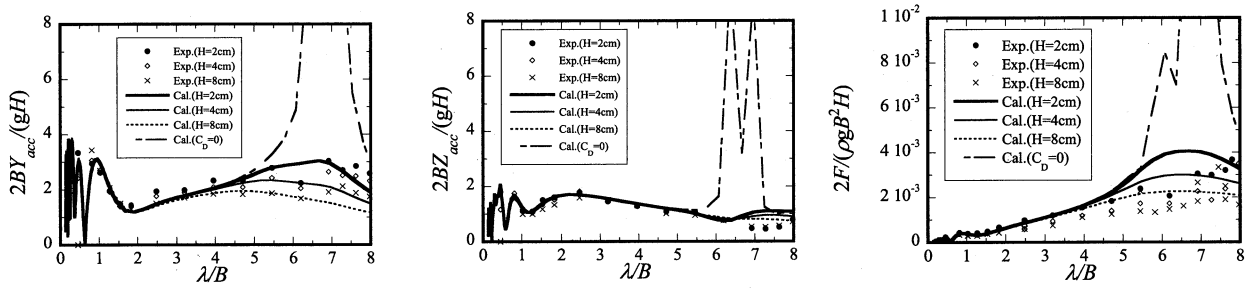

(a) Horizontal direction (b) Vertical direction

Fig. 8 Comparison of mooring forces

Fig. 7 Comparison of acceleration responses

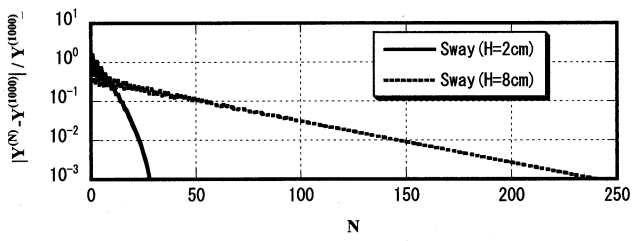

Fig. 9 Example of a convergence of a solution (T=2.5s, Sway)

modes because the non-linear damping effect becomes small.

SAFETY OF THE PROTOTYPE FLOATING STRUCTURE

Random wave induced motion analysis was performed for a prototype floating structure which is located at water depth of 100m. Oceanographic conditions are two cases shown in Table. 2, i.e. at "extreme wind speed condition" which corresponds to wind speed of 50 year recurrence period and "operational wind speed condition" which corresponds to the rated wind speed of a wind turbine. Safety of the mooring system and stability of the wind turbine in terms of tilting angle were investigated for the former and latter conditions, respectively.

At first, mooring stiffness was determined for the wave motion analysis based on a result of catenary analysis from the steady forces, i.e. tidal current force, wind force and wave drift force. As wave directions, see Fig.2 for its definition, three directions, i.e. 30, 60 and 90 degrees were chosen taking account of the symmetry of the structure and the direction of tidal current and wind direction were set as 90 degrees.

Figure 10 demonstrates spectra of incident wave and the response at the

Table 2. Oceanographic conditions

		Operational wind speed	Extreme wind speed
Wave	$H_{1/3}$(m)	3.9	12.0
	$T_{1/3}$(m)	7.4	13.4
Wind speed (m/s)		14.0	50.0
Current speed (m/s)		2.0	

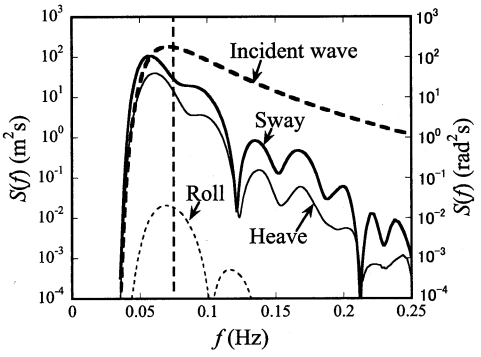

Fig. 10 Spectra of incident wave and responses of the prototype floating structure

storm wind speed condition with wave direction of 90 degrees. Since the natural periods of each mode are considerably larger than the significant wave periods, minimum peaks in the response spectra appear lower period side than the peak period of the incident wave

spectrum. Table.3 demonstrates significant values of the response.

Table 3. Response to each oceanographic condition

		Operational wind speed			Extreme wind speed		
Wave Direction		30°	60°	90°	30°	60°	90°
Response Amplitude (Significant value)	Surge(m)	0.27	0.21	0	2.03	1.13	0
	Sway(m)	0.16	0.37	0.31	1.82	2.68	3.46
	Heave(m)	0.17	0.22	0.16	1.88	1.83	1.97
	Roll(deg.)	0.12	0.22	0.22	1.43	2.28	2.69
	Pitch(deg.)	0.21	0.22	0	2.49	1.84	0
	Yaw(deg.)	0.01	0.18	0	0.08	1.19	0

Mooring force at the extreme wind condition are 4,000kN/line for steady component and 3,700kN/line for the maximum dynamic component which is 1.8 times of significant value and totally 7,700kN/line. It is ascertained that the maximum mooring force is within the failure load of the chain (diameter ϕ=114) 8,895kN. However, in order to keep larger safety factor, it is necessary to increase the diameter of the chain or to increase the number of the lines.

Tilting angle of the floating structure at the operational wind speed condition are 1.2 and 0.4 degree for the static and the maximum dynamic component which corresponds to 1.8 times of the significant value, respectively. It was also ascertained that its value is small enough to keep the operation of power production efficiently.

FATIGUE ANALYSIS

Wind and Wave Climate

It is necessary to consider the combination of 7 parameters from meteorological and oceanographic conditions, i.e. wind speed, wind direction, wave height, wave direction, wave period, current speed and current direction. However it is too complex to take into account all of the combinations. Therefore, in the following analysis, a simplified procedure is applied, i.e. at first, 14 representative wind speeds were determined from cut-in speed to 1 year expected value of 600s mean wind speed. Then wave height and wave period were determined based on the following formula.

Significant wave height was approximated by the SMB formula, in which fetch was modified as a function of wind speed.

$$H_{SMB}(U_{10}) = \frac{0.3\left[1-\left\{1+0.004\sqrt{gF(U_{10})/U_{10}^2}\right\}\right]}{g}U_{10}^2 \qquad (7)$$

Wave period is well approximated as a function of significant wave height specified in the rules and guidelines of Germanischer Lloyd Wind Energie (2005) which is based on full developed JONSWAP spectrum.

$$T_{1/3} \approx 14\sqrt{H_{1/3}/g} \qquad (8)$$

Where $H_{1/3}$ is significant wave height, H_{SMB} is significant wave height by SMB formula, $T_{1/3}$ is wave period, U_{10} is hourly mean wind speed at 10m above the sea surface and F is fetch. Figure 11 demonstrates agreements between approximation by eqs (7), (8) and values from the statistical database of winds and waves around Japan which is edited by Tsujimoto and Ishida (2005). In the wind speed range lower than 10m/s, wave height shows constant value. Therefore significant wave height is determined from eq.(9).

$$H_{1/3} = \max[1.5, H_{SMB}(U_{10})] \qquad (9)$$

Wind direction, wave direction and current direction are demonstrated in Fig.12. Since those are almost collinear, in the following fatigue analysis they are represented by 225 degree which is a predominant direction of current.

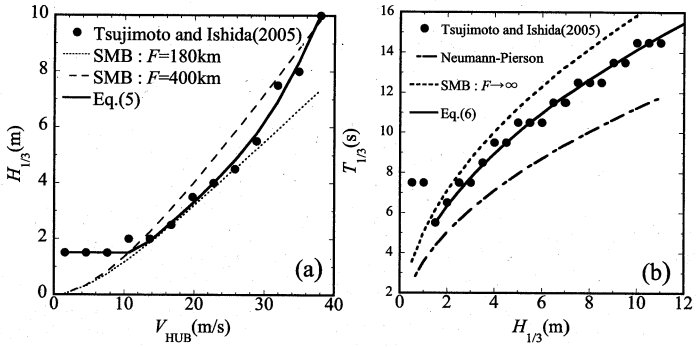

Fig. 11 Wave parameters. (a)Relation between wind speed and significant wave height, (b)Relation between significant wave height and wave period

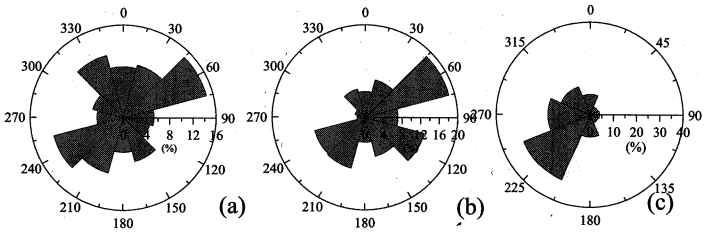

Fig. 12 Wind and wave climate. (a)Wind direction, (b)Wave direction and (c)Current direction

Fatigue Analysis Procedure

Fig.13 demonstrates the steps of fatigue analysis. Steady force is calculated for wind, current and wave drift force. Then the spring constant of the mooring is calculated. Next, motion analysis is performed on the frequency domain using the fluid forces obtained from the Green's function method. Obtained results are transformed into time series by inverse Fourier transform. Based on these data, stress analysis is performed to calculate time series of nominal stress. Numbers of stress cycles are counted by the rainflow counting method. At last long-term fatigue damage is predicted by the linear damage accumulation hypothesis, i.e. Palmgren-Miner's rules together with standard S-N curves. For fatigue analysis, only fluid forces are used for fluctuating force and effect of dynamic loading from wind turbines are not taken into account.

Result of Fatigue Analysis

For fatigue verification, the S-N curve defined by recommendation practice of DNV (Det Norske Veritas 2004, 2005) was used. Structural detail was assumed to be a butt welded tubular joint which is finished its toe by grinding in seawater with cathodic protection, therefore S-N

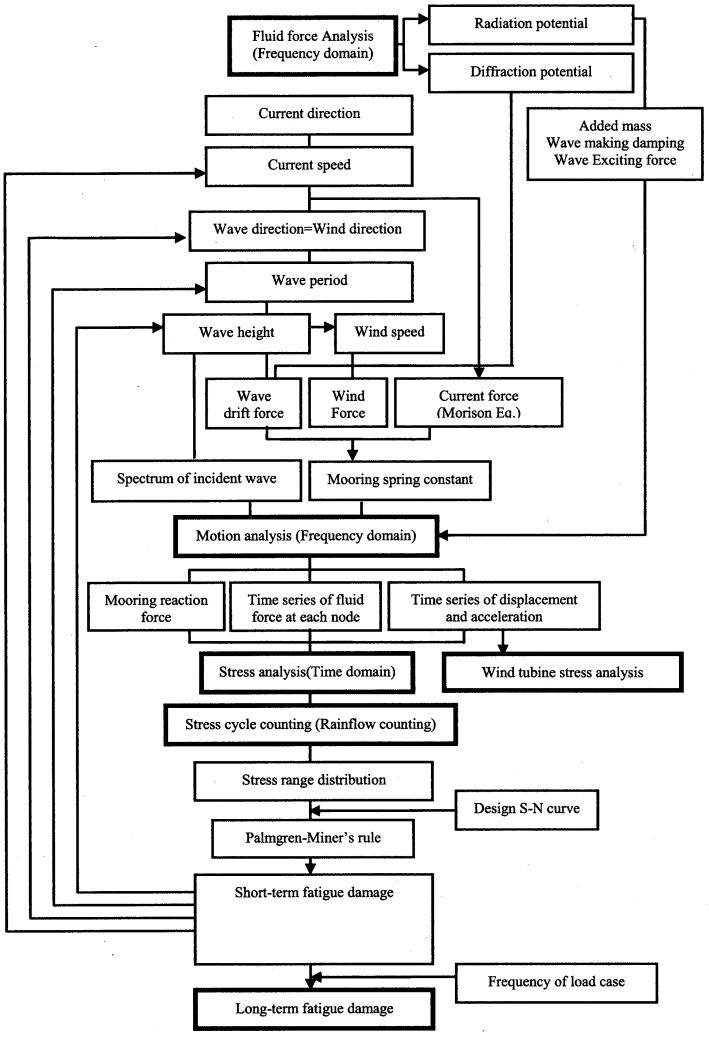

Fig. 13 Steps of fatigue analysis

curve of Class-C was chosen. Partial safety factor for material was chosen as 1.25. Fatigue damages were calculated for 20 year life time. As a result of the fatigue analysis, it is ascertained that the structure has enough strength for fatigue, however, it can be found that fatigue damage is serious at the connection between the connecting girder and WBF. As an example, Fig.14 demonstrates the result of stress cycle counting. From the figure, it can be recognized that the most part of the stress range belongs to the high cycle fatigue range over 10^4.

CONCLUSION

A new light weight semi-submersible floating structure which reduces the wave induced motion was proposed for a support structure of an offshore wind energy conversion system. Its dynamic performance was investigated by the numerical analysis and the model test. The results are summarized as follows:

Characteristics of the wave induced motion can be evaluated in a good accuracy by incorporating the effect of drag force in addition to ordinal Green's function model.

Since the wave induced motion of the floating structure is suppressed small because its natural periods are large, safety of the mooring system at extreme wind speed condition is satisfactory and the tilting angle was ascertained to be small enough to maintain the power production of wind turbine efficiently.

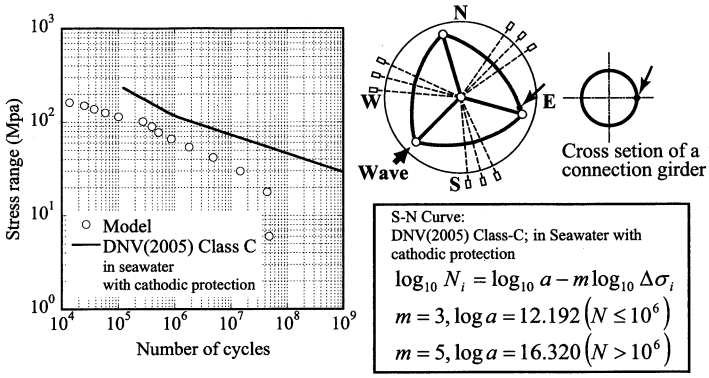

Fig. 14 S-N Curve and the result on number of cycles of stress in connection girder.

Currently, it is ascertained by structural analysis that the cable system which connects connecting girders and CBF contributes to reduce the stress at joints between connecting girders and WBF. This result and optimization of the structure will be reported in another opportunity.

ACKNOWLEGEMENTS

The authors would like to thank to Kiyokazu Yago and Yutaka Ohkawa of National Maritime Research Institute for their suggestion and guidance for the experiments.

REFERENCES

Architectural Institute of Japan (1990). "Recommendation for Structural Design of the Oceanic Architecture (Floating-Type Structure)," pp 110-118.

Det Norske Veritas (2004). "Design of offshore wind turbine structures, " Offshore Standard DNV-OS-J101.

Det Norske Veritas (2005). "Fatigue design of offshore steel structures, " Recommended Practice DNV-RP-C203.

Germanischer Lloyd Wind Energie (2005). " Rules and Guidelines, IV Industrial Services, 2 Guideline for the Certification of Offshore Wind Turbines, " Appendix 4.J, pp 4-73.

Japan Oceanographic Data Center (1991), "Statistical chart of tidal current around Japan (in Japanese)," JP011-91-1, pp 58-61.

New and Renewable Energy Division, Ministry of Economy, Trade and Industry (2001), Summary of the report by the New and Renewable Energy Subcommittee, Conception of Future New Energy Measures, pp 4 (http://www.meti.go.jp/english/report/index.html)

Ohyama, T, Tsuchiya, M (1997). "Expanded mild-slope equations for the analysis of wave-inducd ship motion in a harbor," *Coastal Engineering*, No 30, pp 77-103.

Seto, H (1991). "Efficient evaluation of some singular integrals appearing in multipole expansions in water of finite depth," Trans. of the West-Japan Soc. of Naval Arch., No. 83, pp 103-113.

Seto, H (1992). "Some expressions of pulsating source potentials in shallow water and their efficient algorithms, " Trans. of the West-Japan Soc. of Naval Arch., No. 85, pp 25-36.

Sukegawa, H, Ishihara, T, Yamaguchi, A, and Fukumoto, Y (2006). " An Assessment of offshore wind energy potential using mesoscale model, " *Proc European Wind Energy Conference* 2006, EWEC, Athens, BL3.281.

Takayama, T, Nagai, T, Kikuchi, O, and Moroishi, K (1980). "Motions

and Mooring Forces of a Rectangular Floating Body in waves (1st report) , " Report of the Port and Harbour Research Institute, Vol. 19, No. 3, pp 71-103.

The Japan Machinery Federation and Japan Ocean Industries Association (2002). "Report on the investigations of the development of offshore wind power and other energy conversion systems for the use of ocean resources and energy (in Japanese), " pp40-129.

Tsujimoto, M, Ishida, S (2005). "Statistical characteristics of winds and waves around Japan," Proc. of 15th ISOPE, Vol.3, pp 108-115.

Wehausen, JV, and Laitone, EV (1960). "Surface waves, " Encyclopedia of Physics, ed. S. Flugge, Vol.9, Fluid Dynamics III, Springer-Verlag.

APPENDIXES

Calculation of significant values and time series of the response

Significant values of the response are obtained as follows by assuming that the fluctuation of the response is Rayleigh distribution,

$$\left(\xi_j\right)_{1/3} = \left(0.25\pi\sigma_{\xi_j}^2\right)^{1/2} \tag{6}$$

where $\sigma_{\xi_j}^2$ is variance of the response and is obtained from response spectra. Time series of the responses are obtained by inverse Fourier transformation using response spectrum and phase spectrum.